

# Rapid assessment of abrupt urban mega-gully and landslide events with Structure-from-Motion photogrammetric techniques validates link to water resources infrastructure failures: in an urban periphery

Napoleon Gudino-Elizondo<sup>1,2,3</sup>, Matthew W. Brand<sup>2</sup>, Trent W. Biggs<sup>3</sup>, Alvaro Gomez-Gutierrez<sup>4</sup>, Eddy Langendoen<sup>5</sup>, Ronald Bingner<sup>5</sup>, Yongping Yuan<sup>6</sup>, Brett F. Sanders<sup>2</sup>

<sup>1</sup>Instituto de Investigaciones Oceanológicas, Universidad Autónoma de Baja California, Ensenada, 22760, México.

<sup>2</sup>Department of Civil and Environmental Engineering, University of California, Irvine, 92697, USA.

<sup>3</sup>Department of Geography, San Diego State University, San Diego, 92182-4493, USA

<sup>4</sup>Research Institute for Sustainable Territorial Development, University of Extremadura, Cáceres, Spain

<sup>5</sup>National Sedimentation Laboratory, Agricultural Research Service, USDA, Oxford, 38655, USA

<sup>6</sup>U.S. Environmental Protection Agency, Office of Research and Development, Research Triangle Park, Durham, 27711, USA

Correspondence to: Napoleon Gudino-Elizondo ([ngudino@uabc.edu.mx](mailto:ngudino@uabc.edu.mx))

**Abstract.** ~~Mega gullies and landslides pose significant hazards to urban development on steep terrain. Water resources infrastructure failures (WRIFs), such as leaks and breaks in water supply pipes, have been postulated as a trigger of mass~~ Mass movement events but data for validation has been challenging to acquire since earthwork proceeds quickly after events to repair roads and other infrastructure. Urban development in Tijuana, Mexico was monitored for a five-year period to document hazards in the occurrence of mega-gullies and landslides, including sediment volumes. A pose significant risks in urbanizing areas, yet are poorly documented. To obtain primary data on the size, frequency and triggers of abrupt mega-gullies and landslides in urban areas, rapid assessment approach was developed methods based on photogrammetric observations from an unmanned aerial vehicle (UAV) and Structure from Motion (SfM) digital processing photogrammetric techniques were developed and deployed over a five-year period in Los Laureles Canyon, a rapidly urbanizing watershed in Tijuana, Mexico. Three hazardous mass movement events abrupt earth surface hazards were observed including two mega-gullies and one landslide. Furthermore, and all three events were linked to WRIFs. Frequency analysis points to the annual probability a combination of a WRIF-based rainfall and water resources infrastructure failures (WRIFs): (1) water main breaks resulted from rainfall-driven gully erosion event in the range of 40-60%, which is far higher than design levels typically used for that undermined supply lines, and the resulting water jets caused abrupt mega-gully formation; we provide the first-ever detailed documentation of this process in an urban stormwater infrastructure (5-10%). Additionally, sediment modelling points to WRIF-based erosion as environment; (2) antecedent saturation of a hillslope from a leaking water supply pipe contributed to an abrupt landslide during a storm event. The return period of the storms that triggered the WRIFs was ~1-2 years, suggesting that such triggering events occur frequently. WRIF-based earth surface hazards were also a non-negligible contributor to sediment generation. These at the watershed scale. While the number of observed events is small, these results suggest that

Style Definition: Default Paragraph Font

Formatted: Superscript

Formatted: Italian (Italy)

Formatted: Hyperlink, Italian (Italy)

Formatted: Italian (Italy)

Formatted: English (United States)

~~WRIFs are a significant contributor to erosion hazards facing WRIF can, in some cases, be the single most important process generating abrupt and life-threatening earth surface hazards on the poor urban development on steep terrain, and call for expanded monitoring to characterize the occurrence and modes of WRIF-based erosion events. periphery. Future studies of the triggers and mechanisms of abrupt urban mega-gullies and landslides should consider the role of WRIFs in antecedent saturation and erosion by broken water supply lines.~~

## 1 Introduction

Mega-gullies and landslides ~~pose~~ are significant ~~earth surface hazards to~~ urban ~~development areas, particularly in~~ ~~marginalized neighborhoods~~ on ~~steep terrain~~ the periphery of large cities in low- and middle-income countries (Sidle et al., 2011; Anderson et al., 2014; ~~Makanzu Imwangana et al., 2014; Fu et al., 2020~~). Mega-gullies ~~are erosional features with widths and depths of several meters, while~~ and landslides ~~are downslope mass wasting under the influence of gravity. Both mass movement mechanisms~~ can undermine or damage housing and civil infrastructure, ~~while landslides~~ and present life-threatening safety risks (Calvello et al., 2016; Peng et al., 2017; McAdoo et al., 2018). ~~Mega-gully and landslide hazards are increasing at a time of rapid urbanization as a result of limited oversight of planning and construction as well as socio-economic pressures that force populations to settle in high-hazard areas (Hardoy et al., 2013; Retief et al., 2016; Miller et al., 2019). Moreover, mass movement hazards are concentrated in developing middle and low income regions of the world where unregulated settlement occurs on steep slopes (Anderson et al., 2014).~~ For example, in Latin America, ~~expanding poor areas~~ urban expansion on the periphery ~~of large cities often~~ ~~happens~~ occurs on steep slopes (Sepúlveda and Petley, 2015), ~~and unregulated expansion often results in poorly planned and/or poor unmaintained~~ infrastructure that is vulnerable to erosion and destabilization (Griffin and Ford 1980; ~~Davis, 2006~~ Kjekstad and Highland, 2009; Biggs et al., 2010, 2014; Bianchini et al., 2017; Costa et al., 2018; de Albuquerque et al., 2020).

~~Successful hazard mitigation requires understanding~~ Earth surface hazards that occur abruptly are of ~~mechanisms~~ particular concern from a safety and triggers. ~~In damage perspective, because there is little time for warnings and other emergency response measures. The literature characterizes the~~ ~~formation~~ of urban mega-gullies, ~~the dominant mechanisms identified in the literature relate to surface runoff generated by rainfall during storm events, exacerbated by flow path concentration on road networks (Imwangana, as gradual, occurring over periods of years or more, and as a result of landscape changes such as deforestation, roads, and urban development (Archibold et al., 2014). The role of rain generated runoff in gully formation has been highlighted in studies of 2003; Adediji et al., 2013; Makanzu Imwangana et al., 2015; Zolezzi et al., 2018). In both agricultural and urban areas, area, gully formation is associated with rain-generated runoff (Valentin, et al., 2005). However, mega-gullies may also form abruptly in the presence of a high velocity water jet from a pressurized pipe, a process similar to hydraulic mining used in mining operations in California during the 19th century (Gilbert, 1917). Furthermore, under rapid urbanization with limited oversight of design and construction, water supply systems are vulnerable to breaks that trigger hydraulic mining and the abrupt formation of mega-gullies on time scales of hours to days. In~~

Formatted: Indent: First line: 0.5"

Formatted: English (United States)

Formatted: English (United States)

Formatted: English (United States)

Tijuana, Mexico, local authorities have observed hazardous mega-gullies from pipe breaks and hydraulic mining (Chief of Civil Protection, Tijuana Mexico, personal communication, 2016), but the phenomenon has not been documented in the literature. Landslides may also occur abruptly. Landslides refer to a wide range of phenomena associated with the downslope movement of earthen material (e.g., rock or soil) under the influence of gravity, but (rotational) soil slides are the most common landslide type and abrupt events have been recognized as a significant threat to public safety (Highland and Bobrowsky, 2008). Landslides occur when the weight of earth material down a landslide hazard, similarly, is thought to be controlled by a combination of inherent slope instability exacerbated by hydraulic erosion (Xu et al., 2015) and exceeds its strength (Highland and Bobrowsky, 2008), a process known as overloading that typically occurs with high soil moisture content following storms/rainfall (Kuo et al., 2018; Valenzuela et al., 2018; Zhuo et al., 2019; Monsieurs et al., 2019; Marino et al., 2020). However, there is increasingRecent studies have also shown that leaky pipes and septic tanks contribute to overloading (Demoulin and Hans-Balder, 2021). In summary, there are multiple lines of evidence that both water resources infrastructure failuresWater Resources Infrastructure Failures (WRIFs) are an important trigger of mass movement and rainfall contribute to abrupt earth surface hazards within urban development on steep slopes. WRIFs include cracks, leaks, and breaks of water supply, drainage and/or sewerage pipes that are buried beneath the ground surface, urbanizing areas. More broadly, WRIFs have been linked to numerous other land surface processes such as the generation of sinkholes (Kim et al., 2018), amplified erosion (Guo et al., 2013), and destabilization of soil (Van Zyl, et al., 2013). Nevertheless, little is known about the frequency and severity of mass movement hazards linked to WRIFs. However, the occurrence of abrupt mega gullies from WRIFs and the interdependence with rainfall has not been a focus of previous research, which cannot be predicted or modelled from geomorphic and hydrologic processes occurring at smaller spatial scales but is necessary to quantify in order to develop a complete description of the socio-geomorphology (Ashmore is needed given the threat of fatalities posed by abrupt hazards and the global growth of urban areas in the Anthropocene (Criqui, 2015) of rapidly urbanizing regions.; Ercoli et al., 2020). Monitoring of mega gullies and landslides and analysis of abrupt earth surface hazards in urban areas is challenging, as earthwork. Earthwork typically proceeds quickly after an event to clean up or restore sites impacted by displaced sediment, and access within days, the site is often so disturbed that it becomes impossible to perform a detailed investigation including measurement of feature size and identification of triggers. Access for monitoring faces also raises safety concerns related to slope instabilities.

due to the steep and unstable slopes. Structure-from-motion (SfM) photogrammetry can presents a promising new approach to address these problems. SfM can safely monitor mass movement features with either on-ground or airborne platforms (Nadal-Romero et al., 2015; Eltner et al., 2016; Kaiser et al., 2018; Fugazza et al., 2018; James et al., 2019; Ma et al., 2020), and can be deployed quickly after an event to scan a site—providing data that can be subsequently processed to estimate volumes of sediment displaced and the dimensions of erosional features. This paper reports the results of a five-year observational study whereby SfM was deployed in a rapid response mode to document the frequency and magnitude of mass movement hazards associated with WRIFs, and to quantify the amount of sediment generation compared to other processes. To our knowledge, no study has examined the impact of WRIF on hazardous mass movement events and its impacts on

Formatted: Indent: First line: 0.5"

100 sediment budget at the watershed scale (Jonita et al., 2015; Poesen, 2018). The study is conducted in Los Laureles Canyon  
watershed (LLCW), a rapidly urbanizing area of Tijuana, Mexico. Here, construction of housing and roadways on steep slopes  
created conditions conducive to increase soil erosion, sediment generation, slope instabilities and flood hazards (used to  
105 estimate the dimensions and volumes of sediment displaced by erosional features. Furthermore, recent advances in the  
combination of UAS, SfM and MultiView-Stereo (MVS) algorithms facilitate data acquisition and processing to obtain high  
resolution point clouds, Digital Surface Models (DSMs) and orthophotos (Zhang et al., 2019). Biggs et al., 2010, Luke et al.,  
2018, Goodrich et al., 2020). Moreover, local authorities (Chief of Civil Protection, Tijuana Mexico, personal communication,  
2016) have observed that WRIFs trigger mega-gullies and landslides that pose life-threatening hazards. The objectives of this  
paper are three-fold: (1) to report the effectiveness of SfM photogrammetric techniques for rapid erosion assessment following  
WRIF events, (2) to document the frequency and magnitude of sediment mobilization from WRIF events, and (3) to evaluate  
110 the significance of WRIF events with respect to mass movement hazards and sediment budgets at neighborhood- and  
watershed scales.

Herein we present a 5-year observational study whereby SfM was deployed in a rapid-response mode to document  
the frequency and magnitude of abrupt earth surface hazards, to document the relative roles of WRIFs and rainfall in hazard  
formation, and to quantify the amount of sediment generated by the WRIF hazards compared to other rainfall-runoff processes.  
115 The study is conducted in Los Laureles Canyon watershed (LLCW) located in the urban periphery of Tijuana, Mexico, and  
builds on previous work by the authors to document soil erosion, sediment generation, and flood hazards at the watershed scale  
(Biggs et al., 2010, Luke et al., 2018, Gudino-Elizondo et al., 2019; Goodrich et al., 2020). To our knowledge, no study has  
examined the role of WRIFs in abrupt earth surface hazards, a topic of growing importance in the Anthropocene (Vanmaercke  
et al., 2016 and 2021; Poesen, 2018). The objectives of this paper are three-fold: (1) to provide primary data on size, frequency  
120 and triggers of abrupt mega-gullies and landslides that occur in an urban periphery, (2) to demonstrate a SfM based approach  
suited to the rapid response needs of abrupt earth surface hazards, and (3) to evaluate the significance of WRIF events with  
respect to mass movement hazards and sediment budgets at neighborhood- and watershed-scales.

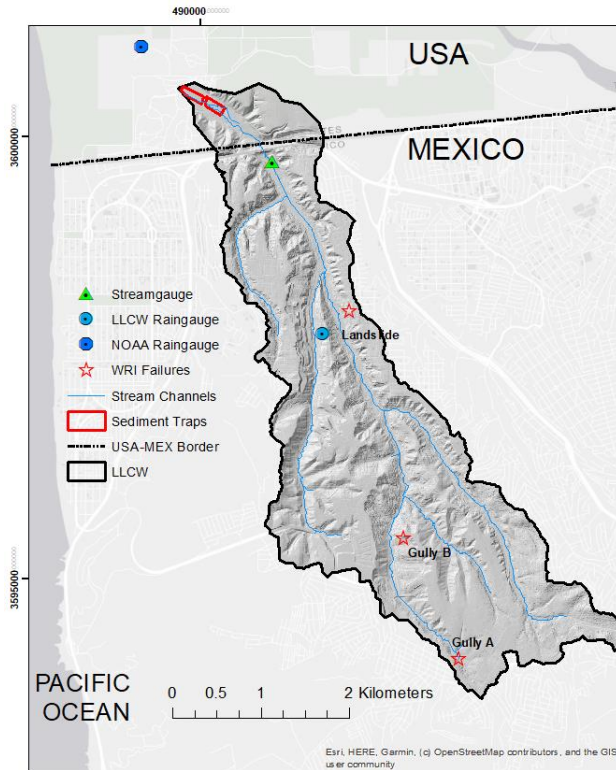
The remainder of the paper is organized as follows: Section 2 (Methods) presents a site description, SfM-based observational  
methods, and watershed modeling methods ~~to for estimating components of the sediment budgets~~ budget; Section 3 (Results)  
125 presents ~~data on SfM and modelling results showing~~ the frequency and magnitude of WRIF-based mass ~~movement and~~  
~~neighborhood~~ and a comparison of WRIF-based fluxes ~~earth surface hazards compared~~ to other mechanisms of sediment  
generation. ~~The paper concludes with discussion~~ Section 4) (Discussion) contemplates the relative contribution of rainfall  
and WRIFs in the observed earth surface hazards, and ~~conclusions~~ (the value of SfM in this context; and major findings are  
reported in Section 5 (Conclusions).

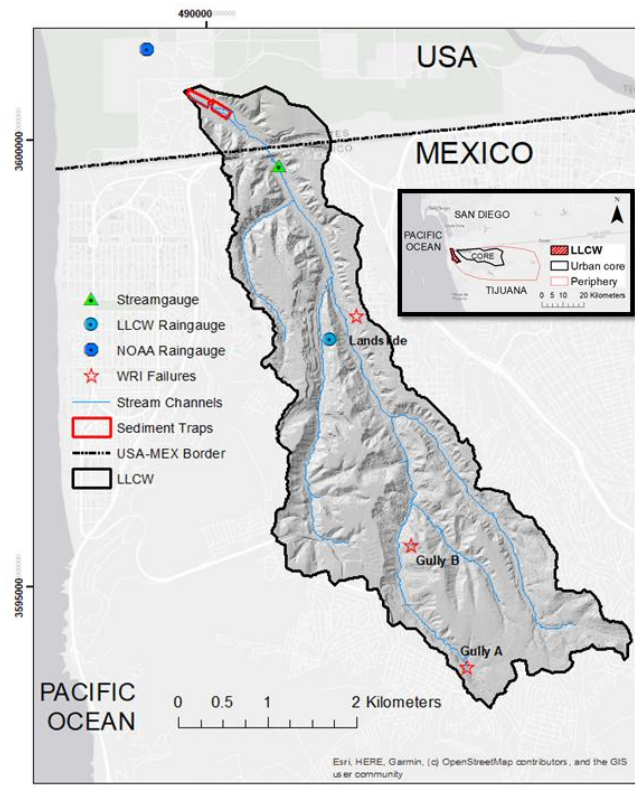
130 **2 Materials and Methods**

**2.1 Site Description**

The Los Laureles Canyon Watershed (LLCW) is ana small (11.6 km<sup>2</sup>) urbanizing binational catchment that overlaps watershed on the western-most portion urban periphery of the USA—Tijuana, Mexico border. (Fig. 1). LLCW flows from the city of Tijuana, Mexico, into the Tijuana River Estuarine Reserve, USA (Fig. 1). Sediment from excess erosion and solid waste transported in Excess sedimentation into the channel network estuary, which is due to high sediment loads from Tijuana, have buried and impaired the estuarine ecosystem (Weis et al., 2001).

135





140 **Figure 1. Los Laureles Canyon Watershed (LLCW), locations of water resources infrastructure failures (WRIFs), and field equipment. [Inset shows the regional location of the LLCW within the urban periphery.](#) Base map from © OpenStreetMap contributors, 2020. Distributed under a Creative Commons BY-SA License.**

145 The climate in LLCW is Mediterranean, with a wet winter, dry summer and an average annual precipitation of 240 mm. The regional geology includes marine and fluvial deposits of conglomerate, sandy conglomerate, and siltstone of the San Diego formation (Gastil et al., 1975, Minch et al., 1984). Soils are generally sandy with a wide range of cobble fraction, and are dominated by steep slopes (15 degrees, average). Urbanization in LLCW started in 1962, with most urbanization occurring between 1980 and 2002 (Biggs et al., 2017), [mostly](#) in the form of unauthorized housing developments (“invasiones”). [Construction](#) [Unauthorized construction](#) of poorly planned housing, [water distribution networks](#) and roadways on steep slopes

150 ~~created conditions conducive to concentrate~~concentrated storm-water runoff and ~~increase~~increased soil and gully erosion, slope instabilities, and failures in WRIF. ~~The~~The LLCW is on the western periphery of Tijuana; the socioeconomic status of residents in the LLCW is low in the southern part of the watershed and in the areas with infrastructure failure as evidenced by a high marginality index and a low fraction of homes with piped water or drainage as compared with other areas of Tijuana (Biggs et al., 2014).

## 155 2.2 Study Design

Hydrologic conditions, slope instabilities, and sediment generation rates were monitored in the LLCW for a 5-year period beginning in January 2013 and ending in April 2018. ~~To measure rainfall, a~~ tipping-bucket rain gauge station ("LLCW raingage" in Fig. 1) was installed in the watershed, and ~~to measure stream stage,~~ a pressure transducer (PT) (Solinst, water level logger) was installed in a concrete channel at the watershed outlet and logged ~~conditions~~water level at 5-minute intervals (Fig. 1). Upon detection of flow at the watershed outlet, field personnel travelled to the site, performed a visual inspection of site conditions, and, upon observation of mega-gullies and landslides, collected two types of data about the WRIF erosional features: (1) photogrammetric surveys (RGB images) were performed ~~with a nonmetric camera (GoPro Hero3+) from using~~ either a ground-based or aerial platform, and (2) ground control points (GCPs) were acquired by differential GPS (Magellan Pro Mart 3) with sub-centimeter to 5 cm accuracy (Magellan Systems Corporation, San Dimas, USA). These primary data were used to create ~~Digital Surface Models (DSMs);~~ and in turn, estimates of sediment volumes and their impacts on sediment budget, as well as to document safety hazards to the people living in the watershed and downstream ecosystems.

165 \_\_\_\_\_A long-term record of rainfall is available from the NOAA Tijuana River Estuary gauging station, located near the outlet of the LLCW, which provides daily rainfall for the period 1980 to 2018, ~~and estimates of daily rainfall back to ~1950 were reconstructed by regression with a nearby gage at Lindbergh airfield in San Diego (Brand et al., 2020).~~ These data are used here to estimate the return period of storm events during the study period. ~~Data~~Gudino-Elizondo et al., (2019) used data from the tipping-bucket rain gauge (LLCW Raingage in Fig. 1) ~~were used~~ to force a watershed erosion model, ~~which was validated with stream gauge data and observed sediment loads at the outlet. The Rates of sediment generation by sheetwash, rill, gully and channel erosion estimated by the model was used to compare~~were compared with sediment generation from WRIF features ~~with the other watershed processes described in section 2.4.~~

## 175 2.3 Image acquisition and processing

Photogrammetric surveys ~~were performed~~ using a ~~modified~~ nonmetric camera (GoPro Hero3+) ~~were completed using with a non-distortion lens (Peau Productions, CA, USA, http://www.peauproductions.com/) mounted~~ either on an Unmanned Aerial System (UAS) (DJI, Phantom2) or a telescoping painter's pole (approximately 2-3 m long). The UAS is advantageous for relatively large and wide erosional features compared with the painter's pole, which can better access relatively small, narrow, and deep erosional features (Gudino-Elizondo et al., 2018a, Taniguchi et al., 2018). Images were acquired once per second

using the time-lapse capture mode from different angles to ensure a high overlap between photographs and to reduce the shade in each image (Castillo et al., 2015) and doming deformations (James and Robson, 2014).

The sediment volume mobilized was estimated using a four-step procedure: (1) Imagery were combined with a subset of the GCPs to calibrate the camera and produce Structure from Motion (SfM) point clouds following general workflows (Agisoft LCC, Russia, Version 1.4.4), (2) SfM point clouds were converted to a digital surface model (DSM) (Agisoft LCC, Russia, Version 1.4.4), (3) erosional volumes were computed (ArcGIS 10.6.1, ESRI, Redlands, California) by subtracting the DSM from a reference DSM representative of the pre-event land surface (Wheaton et al., 2010), and (4) the difference [DSM of DSMs \(DoD\)](#) was integrated to calculate the total sediment volume- ([James et al., 2012](#)). Volumes were converted to mass using a bulk density of 1,600 kg /m<sup>3</sup> corresponding to very fine sand (USDA, 2018).

Pre-event topography was based ~~on~~ either [on](#) a 2014 aerial LIDAR survey (1 m resolution [Digital Surface Model \(DSM\)](#) with a 0.11 m vertical RMSE, NOAA, 2014), or [without](#) UAS-based DSMs generated with imagery collected before the failure event (Table 1). The horizontal and vertical RMSE of the [DSM point clouds](#), or geo-registration error, was estimated using the subset of the GCPs not used to produce the SfM point cloud, called Error Control Points (ECPs). Previous work indicates that 4 to 5 GCPs with a few additional ECPs are adequate for SfM processing (James et al., 2017). The RMSE for the [DSM creation DoD](#) was computed as the square root of the sum of the squared errors for each [ECP DSM](#) (Alfonso-Torreño et al., 2019).

**Table 1. Structure from Motion survey description and data acquisition**

Erosional feature	Landslide	Mega-gully A	Mega-gully B
Acquisition platform	<a href="#">UAVUAS</a>	<a href="#">UAVUAS</a>	Pole
Date of survey	05/22/2015	09/23/2015	02/17/2017
Number of pictures	62	115	899
Altitude (m)	75 m	30 m	4 m
Area covered (m <sup>2</sup> )	38,400	1,800	2,800
Ground sample distance (cm/pxl)	10	4	3
Point density (points/m <sup>2</sup> )	11	48	261
Numbers of GCPs	8	8	12
Numbers of ECPs	6	6	10
<a href="#">RMSE of ECPs (horizontal, vertical) (cm)</a>	<a href="#">(3, 7)</a>	<a href="#">(3, 5)</a>	<a href="#">(3.5, 5)</a>
Pre-event topography	<a href="#">LIDAR-DSM</a>	SfM	SfM

Formatted Table



200 ~~As another check on accuracy, the~~The dimensions of invariant features (concrete pads, water pipes, etc.) were directly measured in the field and compared to length estimates from the SfM point cloud as described in Gudino-Elizondo et al. (2018a). Additionally, pre- and post-event ground elevations were compared along transects outside the disturbed region where no topographic change was observed [to assess co-registration errors of the DoDs calculation](#).

#### 2.4 Watershed Modeling

205 The Annualized AGricultural Non-Point Source (AnnAGNPS) model (Bingner et al., 2015) was applied to the LLCW to simulate discharge and sediment load during storm events and to develop an inventory of sediment generation rates by mechanism at the watershed scale. The AnnAGNPS model was previously calibrated and validated for runoff and observations of sediment generation in LLCW (Gudino-Elizondo et al., 2018a, 2018b, 2019b), and the applications here rely on this calibration. The simulation period was [from water year 2012 to 2017 water years](#) to match the ~~observational~~observation period  
210 [of the mega-gullies and landslide](#). Sediment excavation rates from ~~the~~ sediment traps at the LLCW outlet (Fig. 1) were used for model calibration. The sediment traps were excavated annually from 2007–2012 (N = 7). Uncertainties in the ~~modeled~~modelled sediment yield were previously reported by Gudino-Elizondo et al. (2019b) as approximately 10%, with a normalized RMSE of 48%.

215 \_\_\_\_\_ Measurements and modeling supported an inventory of sediment generation and load from four mechanisms: (1) sheet and rill erosion, (2) gully erosion, (3) channel erosion, and (4) erosion from WRIF. Sediment generation was considered as the total mass of sediment mobilized, while the sediment load was the quantity of sediment observed at the watershed outlet. Sediment load from WRIF was calculated by multiplying the erosion volume per event times the Sediment Delivery Ratio (SDR). For mega-gullies, the SDR was set to 1 based on field observations and modeling work described in Gudino-Elizondo et al. (2019b). Conversely, the SDR was set to zero for the landslide based on field observations that displaced sediment was  
220 intercepted by the road network and mechanically removed or repositioned on the hillslope (Vigiak et al., 2012). Of course, subsequent rainfall events may cause the repositioned sediment to be later mobilized and moved towards the stream network, so our estimates of load correspond only to the period of observation.

#### 2.5 Hazard assessment from water resources infrastructure failure

225 Reports of the damage caused from mega-gullies and landslide were compiled from residents and local agencies. Primary data from the three events are described, including impacts to transportation, housing, urban infrastructure and downstream ecosystems and communities in the study watershed. [The year of urbanization of the neighborhoods where the WRIFs were occurred was determined from an existing dataset \(Biggs et al. 2010\)](#). The specific soil loss (SSL) of the WRIF mega-gullies was calculated as the total erosion (m<sup>3</sup>) normalized by the watershed area (m<sup>2</sup>) and was then compared to the observed SSL in the study watershed and to other studies reported in the literature. A detailed description of safety hazards and the contribution  
230 to the total sediment budget of each WRIF event is described in section 3.

### 3 Results

A total of 14 storm events ~~were~~ observed during the 5-year study period, based on a flow threshold of  $1 \text{ m}^3 \text{ s}^{-1}$  (or  $\sim 15 \text{ cm}$  of water in the channel) at the gaging station, which corresponds to a depth of rainfall ranging from 6.5 to 13 mm. The total depth of the 14 storms was 322 mm, or 35% of the total rainfall (907 mm,  $181 \text{ mm y}^{-1}$ ) for the 5-year period. Mass movement from WRIFs were observed during three of these events, each characterized by a 1-2-year return period. WRIFs leading to mass movement were not observed between storm events or during smaller storm events ( $< 23 \text{ mm}$ ). [Figure 2a shows the reconstructed rainfall time series for the period 1950-2017 which demonstrates variability over roughly seven decades, and Figure 2b shows the timing of WRIF-based mass movement events alongside measured daily rainfall for 2013-2017. Both mega gullies events are associated with rainfall that exceeds the threshold for rainfall-driven gully formation reported by \[Gudino-Elizondo et al. \\(2018a\\)\]\(#\) but is not exceptional in magnitude considering the long term record. The year of urbanization of the neighborhoods was 1980 \(landslide\), 2010 \(mega-gully A\), and 2002 \(mega-gully B\), respectively. Hence, the landslide is associated with a later stage of urbanization \(34 years\) compared to mega-gully A \(4 years\) and mega-gully B \(15 years\).](#)

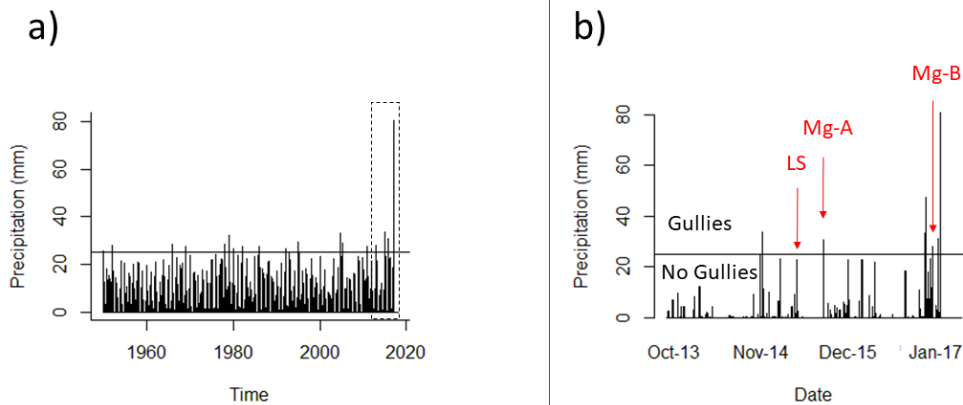


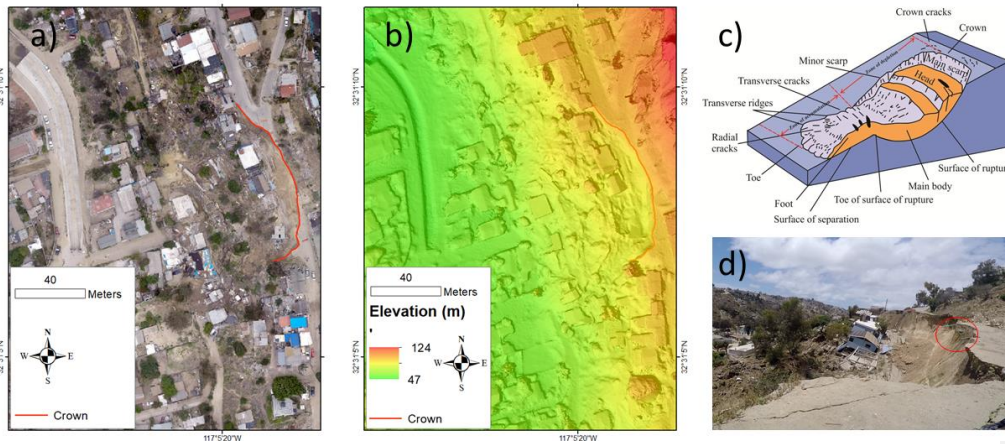
[Figure 2. a\) Reconstructed daily rainfall time series measured at the watershed outlet for 1950-2017, with horizontal line representing the rainfall threshold for rainfall-runoff gullies formation \(\[Gudino-Elizondo et al., 2018a\]\(#\)\); and b\) measured rainfall for 2013-2017 and timing of the observed mega-gullies \(Mg\) and landslide \(LS\).](#)

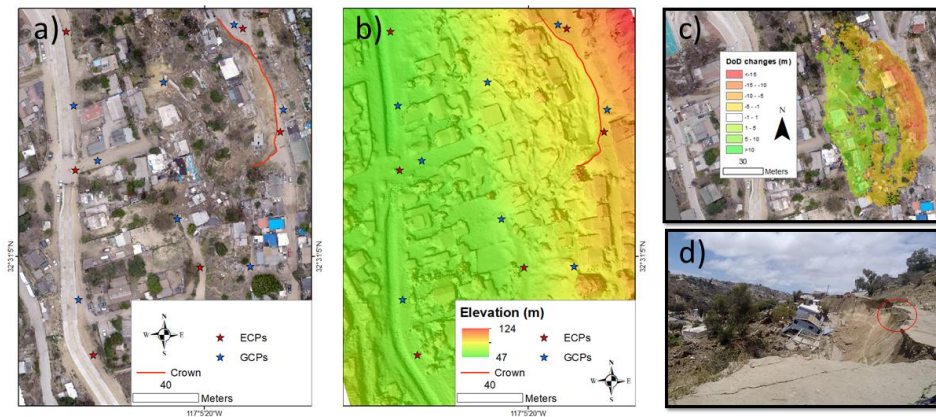
#### 3.1 SfM surveys and social impacts by event

Three storm events caused WRIFs that led to hazardous mass movements. One event involved a landslide and two involved formation of mega-gullies. The detailed observations of each feature are described in sections 3.1.1 to 3.1.3.

### 3.1.1 Landslide

A large [rotational](#) landslide occurred during a storm event on 15 May 2015 (Fig. [23a](#)). More than 20 houses were damaged affecting more than 100 people (Fig. [2b](#), [2e3b](#), [3c](#)). Based on the daily rainfall total (23 mm) and the long-term rainfall record at the NOAA Tijuana River Estuary Gage, the return period of the storm is 1 year. The landslide was attributed to a WRIF based on resident reports that seepage from the slope along with incipient cracks were observed for several days immediately before the failure incident. This observation led to the evacuation of the residents when the evolution of the cracks was evident. The infrastructure failure wetted the soil, and the landslide was then triggered by the rain event. Broken water mains were also observed after the landslide (Fig. [2e3c](#), red circle). The [dimensions of the landslide are main scarp was](#) approximately 20 m high and approximately 75 m long, with a maximum width of 40 m measured from the main scarp to the toe of the hill. SfM photogrammetry leads to an estimate for the sediment volume and mass:  $19,900 \pm 580170 \text{ m}^3$  and  $31,900 \pm 928280$  metric tons. The reported uncertainties ( $\pm$  value) are obtained by propagating [horizontal and vertical RMSEs of individual DSMs in the DSMsDoD calculation](#).





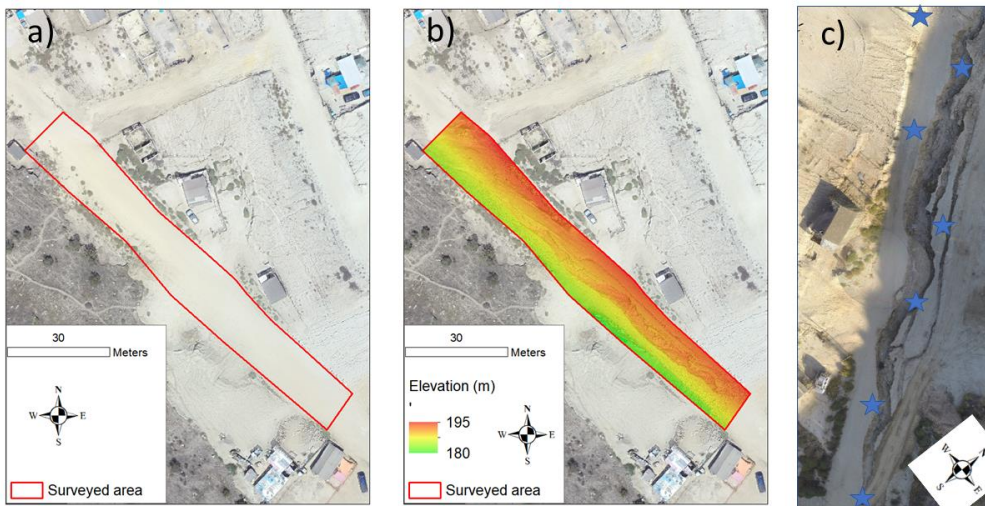
265 **Figure 23.** Landslide event on 15 May 2015 triggered by water main leak and rainfall: (a) Orthophoto acquired after  
the WRIF showing the upper limit of the main scarp (crown) with the red line, and (b) the resulting ~~DEM~~DSM, (c) **a**  
**schematic diagram of DoD changes from the anatomy of a landslide (USGS, 2021), multi-temporal analysis,** and (d) **a**  
ground-based **photographs photograph** of the landslide showing broken water mains inside the red circle aligned with  
the main scarp.

270 The RMSE (ECPs, n=6) of the DSM obtained from SfM was 3 cm in the horizontal and 7 cm in the vertical coordinates. ~~James~~  
~~and Robson (2012) introduced the relative precision ratio for UAS-SfM applications (i.e., ratio of measurement precision to~~  
~~observation distance), and found that 1:950 indicates acceptable accuracy over a range of scales. For a flight height of 75 m,~~  
~~the James and Robson (2012) standard gives a desired DSM error of 7.8 cm, which compares well with the horizontal and~~  
275 ~~vertical errors estimated here.~~ Elevation differences outside of the disturbed area were ~~0.7 cm < 7 cm.~~ Therefore, ~~the co-~~  
~~registration error is assumed to be negligible.~~ The mean difference between measured and ~~modeled~~modelled lengths of objects  
at the site (e.g., sewer manhole covers) was less than 3 cm. These different methods all suggest the error was less than 7 cm  
and within the range expected for the observation distance. ~~The DoD map (Fig. 3c) shows the geometry of the landslide as a~~  
~~deep rotational slope failure, which is consistent with the model proposed by Highland and Bobrowsky (2008) in USGS (2021).~~

### 280 3.1.2 Mega-gully A

~~A mega~~Mega-gully **A** formed along an unpaved road ~~during and immediately~~ following a storm event on 15 September 2015.  
Based on the daily rainfall total (31 mm) and the long-term rainfall record at the NOAA rain gauge, the return period of the  
storm was 1-2 years. This mega-gully was attributed to a WRIF based on resident reports that ~~leakage~~discharge from a broken  
pipe was observed upstream immediately after the failure event (personal communication, Tijuana Metropolitan Planning

285 Institute). In this case, erosion caused by the storm event undermined the water main, which subsequently broke and enlarged the gully as a result of high velocity water jets from the pressurized water main. The mega-gully was 98 m long, with a maximum width of 8 m and maximum depth of 4 m (Fig. 34). The generated sediment mass was estimated as  $1,360 \pm 6535$  tons.



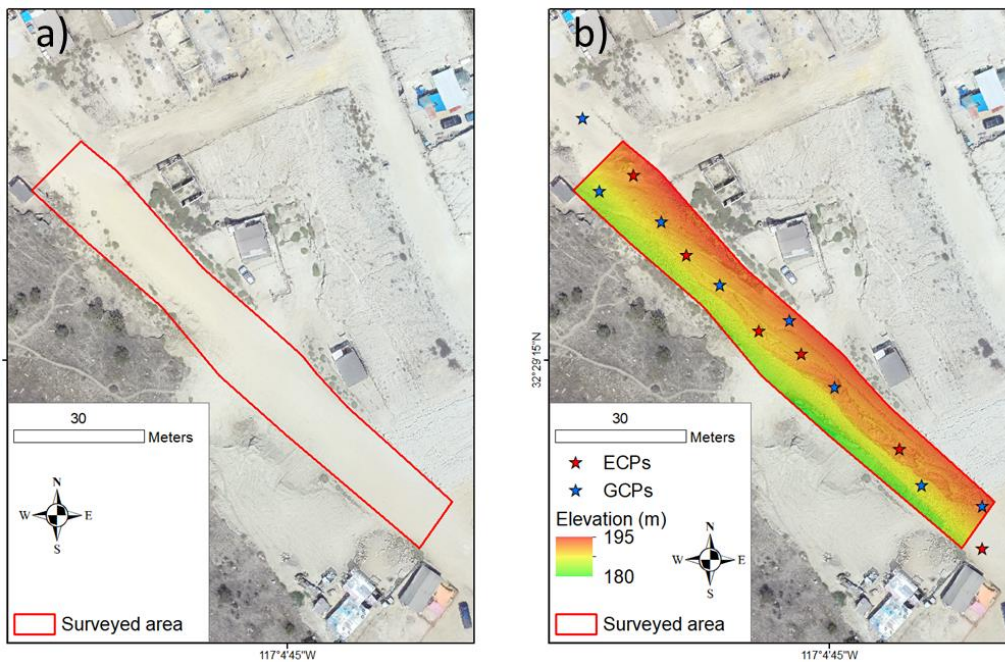
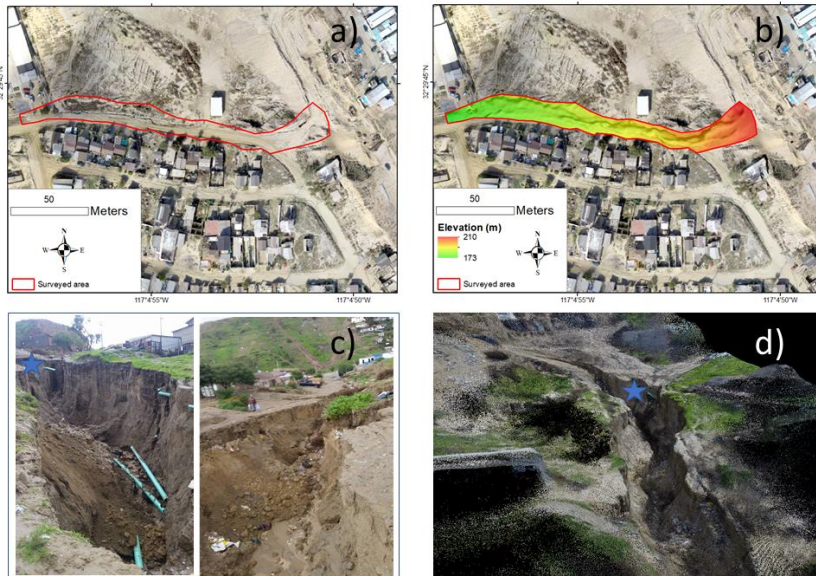


Figure 34. Mega-gully formed on 15 September 15, 2015 by WRIF: (a) Orthophoto acquired before the WRIF showing the extent of the surveyed area centred in the red rectangle, and (b) the resulting DEM and (c) an orthophoto acquired after DSM showing the WRIF, the blue stars represents ground control points, spatial distribution of Ground and Error Control Points (GCPs and ECPs, respectively).

The RMSE (ECPs,  $n=6$ ) of the DSM obtained from SfM was 3 cm horizontal and 5 cm vertical. Elevation differences outside of the disturbed area were 0-5 cm. Field measurements of the mega-gully width and depth differed from the SfM-derived width and depth by less than 2 cm on average. This WRIF caused the interruption of water supply for 1 month, affecting more than 300 residents (personal communication, Tijuana Metropolitan Planning Institute). The corresponding erosional feature impacted public transportation and life quality to the neighbourhood for 6-9 months (available Google Earth imagery 11 December 2015- 08 August 2016) before the road was repaired.

### 3.1.3 Mega-gully B

A second mega-gully (B) formed along an unpaved road (Fig. 5a) following a storm event on 16 December 2016. Based on the daily rainfall total (33 mm) and the long-term rainfall record at the NOAA rain gauge, the return period of the storm is 1-2 years. The mega-gully was largest at the upslope position and decreased in cross sectional area with distance from the broken pipeline. The mega-gully was 202 m long, with a maximum width of 10 m and maximum depth of 7 m. Imagery was collected for the SfM processing using a telescoping painter's pole (Fig. 4d), and sediment generation was estimated to be  $4,340 \pm 408,155$  tons.



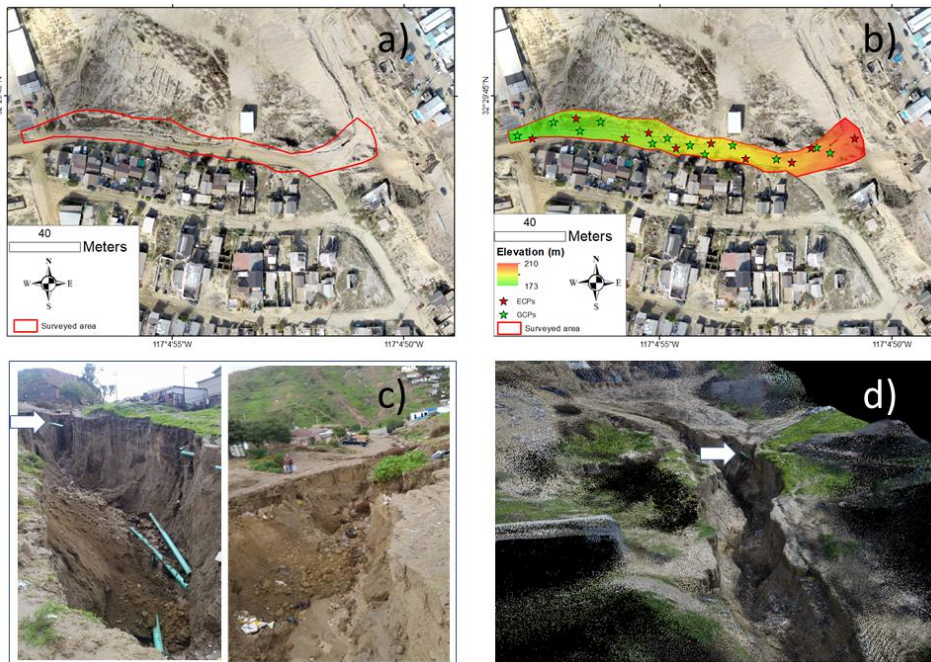


**Figure 45.** Mega-gully formed on 16 December 2016 triggered by WRIF: (a) Orthophoto acquired before the WRIF showing the extent of the surveyed area centred in the red polygon, (b) the resulting ~~DEM~~DSM after the WRIF, (c) Images depicting the mega-gully with view angles looking upslope and downslope of the WRIF, and (d) a screenshot of the resulting point cloud.

The RMSE (ECPs, n=10) of the DSM (Fig. 5b) obtained from SfM was 3.5 cm in the horizontal and 5 cm in the vertical. Elevation differences outside of the disturbed area were 0-5 cm, which is consistent with the accuracy of the method. For example, differences between measured and modelled lengths of not-deforming objects at the site (e.g., water supply pipes shown as blue stars/white arrows in Fig. 4e5c and Fig. 4d5d) were less than 1 cm.

For this second mega-gully event, mass movement was again triggered by erosion that undermined the water main, which subsequently broke and enlarged the gully by discharging piped water directly onto the hillslope. Broken water main pipes were noted during the rapid-response survey (Fig. 4a and 4e5c). The mega-gully also impacted public transportation and life quality in the neighbourhood for 6 months (based on Google Earth imagery) and interrupted water supply for 1 month, affecting more than 200 people (personal communication, Tijuana Metropolitan Planning Institute).



325 **3.2 Comparison of Sediment Generation Sources**

Application of the calibrated AnnAGNPS watershed model to storm events for 2012-2017 yielded daily estimates of rainfall-based sediment generation by sheet and rill erosion, gully erosion and channel erosion. Table 2 presents sediment generation (by mass) on a storm event basis, showing the amount of sediment generation associated with WRIFs measured using SfM, and the simulated total watershed sheet and rill erosion, gully erosion, and channel erosion at the event-scale. Additionally,

330 Fig. 56 shows the relative contribution of WRIF and rainfall-based sediment generation mechanisms.

**Table 2. Sediment generation by process during storm events with WRIFs in the Los Laureles Canyon Watershed.**

<u>Erosional hazard event</u>	<u>Sediment Generation Mechanism (tons)</u>	<u>Landslide event (May 15, 2015)</u>	<u>Mega-gully A event (September 15, 2015)</u>	<u>Mega-gully B event (December 15, 2016)</u>		
<u>*Water Resources Infrastructure Failures</u>	<u>31,900-Measured</u>		<u>1,360-Modeled</u>	<u>Total 4,340</u>		
<u>Water Resources Infrastructure Failures</u>	<u>Water Resources Infrastructure Failures</u>	<u>Channel Erosion</u>	<u>**Sheet and Rill</u>	<u>Rainfall-runoff gullies</u>	<u>4,710</u>	<u>12,100</u>
<u>Landslide **</u>	<u>31,900 ± 280</u>	<u>7,610</u>	<u>5,310</u>	<u>10,500</u>	<u>55,300</u>	<u>49</u>
<u>Rainfall runoff gullies</u>						
<u>*Mega-gully A Channel Erosion</u>	<u>1,360 ± 357,610</u>	<u>2,290</u>	<u>4,710</u>	<u>49</u>	<u>8,410</u>	
<u>Mega-gully B Total Generation</u>	<u>4,340 ± 155,300</u>	<u>5,910</u>	<u>12,100</u>	<u>160</u>	<u>22,500</u>	

\*Sediment quantified using field measurements, \*\*Sediment quantified using the AGNPS model.

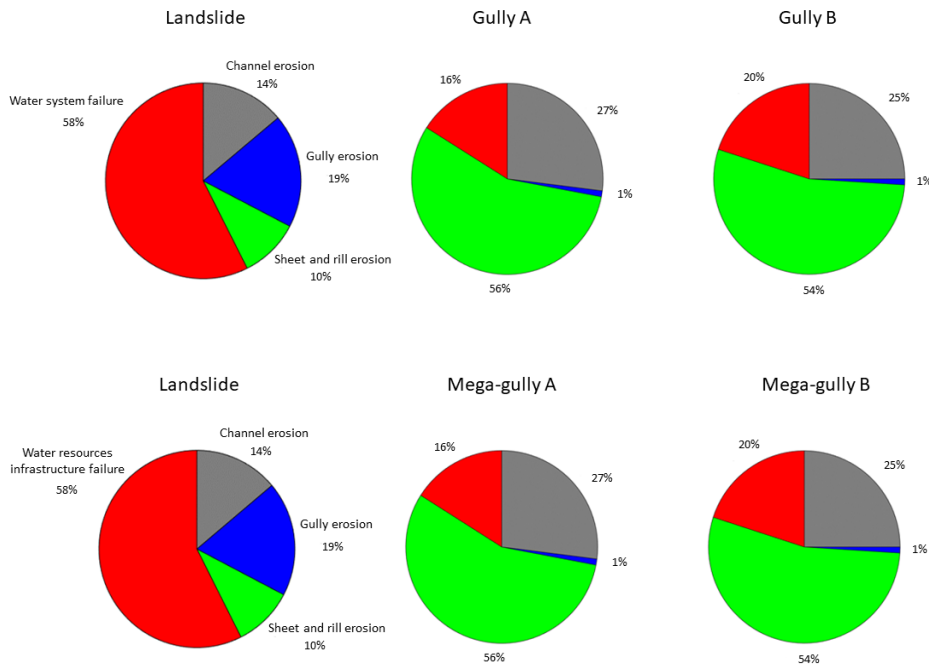
- Deleted Cells
- Formatted Table
- Deleted Cells
- Deleted Cells
- Inserted Cells
- Formatted: Centered
- Merged Cells
- Formatted: Left, Line spacing: single
- Formatted: Centered
- Merged Cells
- Formatted: Font: Not Bold
- Deleted Cells
- Inserted Cells
- Inserted Cells
- Inserted Cells
- Formatted: Centered
- Inserted Cells
- Formatted: Centered
- Formatted: Font: Bold
- Formatted: Centered
- Inserted Cells
- Inserted Cells
- Formatted: Centered
- Inserted Cells
- Formatted: Centered

335

This analysis shows that mass movement associated with WRIFs was significant on an event basis. Mega-gully B generated 4,340 tons (Table 2), which is approximately 80 times the area-normalized annual erosion rate for gullies (tons/ha) and 10 times the total sediment generated by other rainfall-generated gullies (Gudino Elizondo et al., 2018a, Gudino Elizondo et al.,

2018b). The WRIF-triggered landslide mobilized more sediment than all of the rainfall-based processes combined, while the  
 340 mega-gullies triggered by pipe failures and hydraulic mining were responsible for 16 and 20% of the total sediment generation  
 across the watershed (Fig. 56).

The proportion of sediment generated by each erosional process differed markedly between the landslide event and the two  
 mega-gully events (Fig. 56); rainfall-generated gullies contributed more sediment during the landslide event because peak  
 discharge, the main control on gully formation, was higher during the landslide storm event (19.5 cms at the outlet) than during  
 345 the two mega-gully events (~5 cms) (Gudino-Elizondo et al., 2019b).



350 **Figure 56.** Relative contribution of sheet and rill erosion, gully erosion, channel erosion and water system resources  
infrastructure failure (WRIF) towards sediment generation for three storm events with water resources  
infrastructure failures WRIF.

The total sediment generation and load were computed for the 5-year study period by integrating over all storm events (Table  
 3). On a five-year basis, WRIFs contributed 5% of the total sediment generation and approximately 2% of the total sediment

355 load at the watershed scale. While the sample size here is small, the frequency of WRIF-based erosional events can be  
 estimated in several ways: three hazard events occurred over a period that had 14 rainfall events (21% of rainfall events), two  
 out of five years had at least one hazard event (40% chance per year), or three events occurred in five years (60% chance per  
 year). The small sample size implies a high degree of uncertainty in all of these estimates; nevertheless, these rates of  
 occurrence are far higher than typical design standards for water resources infrastructure in urban areas. For example, large  
 360 flood control channels are typically designed with a 0.2-2% annual exceedance probability, and smaller drainage systems in  
 urban areas are often designed for 5-10% annual exceedance probability. Hence, WRIF-based hazards observed during this  
 study are many times more frequent (21-60%) than typical design standards for flood control systems in urban areas (0.2-10%)  
 and thus deserving of greater attention for public safety, infrastructure resilience and environmental protection.

365

**Table 3. Five-year total sediment generation and load rates (by process), fraction of total generation, and fraction of  
 370 total load for the Los Laureles watershed.**

Generation Mechanism (+tons)	5-years Total Sediment Generation (tons)	5-years Total Sediment Load (tons)	Fraction of Total Generation (%)	Fraction of Total Load (%)
WRIF	37,566	5,696	5	2
Sheet and Rill	258,592	197,538	34	48
Rainfall-runoff gullies	228,207	75,253	30	18
Channel Erosion	234,150	131,212	31	32
Total	758,515	409,699	100	100

### 3.3 Comparison to [Previous Observations](#) Other Erosional Features

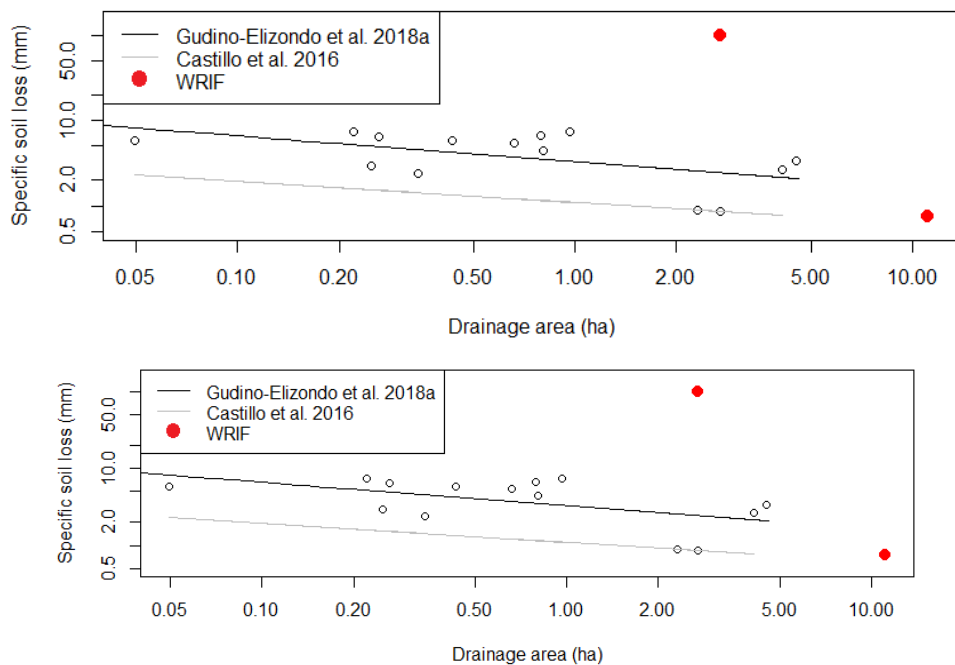
The mega-gullies observed here are large compared to rainfall-generated gullies surveyed in the study area (Gudino-Elizondo  
 et al., 2018a), which had a mean gully width of 1.5 m and a mean depth of 0.5 m. In [contrast terms of size](#), mega-gully A is up  
 375 to 8 m wide and 4 m deep, and mega-gully B is up to 10 m wide and 7 m deep. Mega-gullies A and B are also long with lengths  
 of 100 and 200 m, respectively. Mega-gullies A and B were also more developed than rainfall-generated gullies, with greater  
 connectivity to the stream channel, which enhances sediment delivery to the stream network. [Figure 7 presents an aerial image  
 which provides a visual comparison of mega-gully B to a rainfall-driven gully network on a neighboring unpaved road.](#)

Figure-6



**Figure 7. High-resolution photograph showing the contrast between gullies generated by rainfall-runoff only (road on left) and mega-gully B (road on right).**

**Figure 8** shows that the specific soil loss (SSL, the average depth of soil loss in the watershed) from mega-gully B was exceptionally high compared to rainfall-runoff gullies in the LLCW (Gudino-Elizondo et al., 2018a) and compared to sites reported by Castillo and Gómez (2016), which included sites spanning different land uses and precipitation regimes. The SSL from mega-gully A was comparable to other gullies observed in the study watershed, which has higher rates of SSL than the set of sites reported by Castillo and Gómez (2016).



**Figure 68.** Specific soil loss of mega-gullies caused by WRIF (red dots) compared to previously reported gullies in Tijuana, Mexico (circle points and black line, Gudino-Elizondo et al., 2018a) and trends for ephemeral gullies reported from other sites (gray line, Castillo and Gómez 2016).

395

The landslide caused by the WRIF was the single largest erosional feature observed in the watershed during the study period. Landslides occur throughout Tijuana, with more than 40 landslides from 1992-2012, including –a landslide that damaged 19 buildings (Oliva-González et al., 2014), which is comparable to the LLCW slide (20 buildings damaged). However, data describing the sediment displaced by these 40 landslides and potential connections to WRIFs were not available. [More research is needed to establish the links between WRIFs and landslides.](#)

400

## 4 Discussion

### 4.1 Rapid methods for monitoring erosional features

405 Landslides and mega-gullies have complex topographies and are poorly suited to the application of traditional surveying techniques such as total stations, but are well suited to photogrammetric characterization using SfM. [SfM photogrammetric techniques have been widely used to quantify geomorphic changes in many environments with equivalent resolution compared to more sophisticated topographic techniques \(i.e. TLS, LIDAR\). Accuracies, limitations and disadvantages of both SfM and DoDs applications have been widely described in the existing literature \(Wheaton et al., 2010; James et al., 2012; Carrera et al., 2020\).](#) In our study, photogrammetric data were effectively captured for mega-gullies roughly 5-10 m wide, 5-10 m deep, and >100 m long using a camera mounted on a telescoping painter's pole, and landslides were safely characterized using a UAS-based platform. [James and Robson \(2012\) introduced the relative precision ratio for UAS-SfM applications \(i.e., ratio of measurement precision to observation distance\), and found that a precision ratio of 1:950 indicates acceptable accuracy over a range of scales. For a flight height of 75 m, the James and Robson \(2012\) standard gives a desired DSM error of 7.8 cm, which compares well with the horizontal \(3 cm\) and vertical \(7 cm\) errors estimated here. The errors in the DSMs were very small \(<=5 cm\) compared to the size of the features \(5-10 m\).](#) The presence of urban infrastructure in photographs (e.g., concrete pads, sewer structures) also presented opportunities for ground control points and accuracy checks. [Elevation differences outside of the disturbed areas were <7 cm, indicating minimum co-registration errors. Errors in sediment volume estimates were also small \(1 to 3%\). The DoD also helped to characterize the landslide as a deep rotational slope failure, consistent with other landslides reported in Tijuana, which are linked with unplanned urbanization on hilltops and enhanced pore pressure induced by uncontrolled water leakage \(Oliva-Gonzalez et al., 2014\).](#) We also note from the DSM analyses that [the terrain slope was associated with the depth of incision of WRIF mega-gullies. Mega-gully B was 2-3 times deeper than mega-gully A, which formed on a relatively flat area. Accuracies achieved from these observations \(i.e., 3-cm horizontal RMSE and 5-cm vertical RMSE\), both from individual point clouds and DoD's calculations,](#) are in line with the needs for [erosion hazards surveys and sediment budget applications \(Dietrich, 2016; Alfonso-Torreño et al., 2019; Ma et al., 2020\).](#) The SfM photogrammetric approach is in many ways ideal for surveying WRIFs because: (1) the camera is lightweight and easily mounted on either a ground-based or aerial platform; (2) SfM requires less field personnel reducing significantly human-based errors and is more time efficient than traditional topographic surveying methods (Carrera-Hernandez et al., 2020); and (3) hardware costs are relatively low. Laser scanning or LIDAR systems could be advantageous compared to photogrammetry in terms of point density and data accuracy, but they are typically quite heavy compared to cameras, require more sophisticated spatial referencing systems (e.g., inertial navigation units), often present occlusion artifacts, and are expensive (Izumida et al., 2017; Mazzoleni et al., 2020). Our study demonstrates that both ground-based and UAS-based photogrammetry allow for rapid documentation of hazardous erosional features with minimal equipment and low labor requirements. [Recent advances in UAS-mounted Real-Time or Post-Processing Kinematic \(RTK, PPK\) georeferencing systems allow rapid mapping over relatively](#)

410  
415  
420  
425  
430

435 [large areas without GCPs \(Zhang et al., 2019\), enhancing the potential for rapid response surveys programs, especially in dangerous and inaccessible terrains.](#)

#### 4.2. WRIFs and the sediment budget

Stochasticity in WRIFs and WRIF-based sediment hazards is high. Failures may or may not happen in any given storm (here we observed 3 failures in 14 storm events), and when failures occur, the volume of sediment generated across three events varied by over an order of magnitude. This makes it difficult to generalize and estimate sediment generation by infrastructure failure for other events lacking field observations. However, the data do allow a first-order estimate of annual-average sediment generation from WRIFs which is useful for sizing sediment basins that protect downstream ecosystems from excess sedimentation and for estimating average-annual excavation costs. [We found in previous research that rainfall-runoff gully erosion rates are higher on steep sandy soils \(Las Flores soil type\) \(Gudino-Elizondo et al., 2019\) and a rainfall threshold to generate rainfall-runoff gullies on those unpaved roads \(>25mm\) was also observed \(Gudino-Elizondo et al., 2018\). Therefore, WRIF mega-gullies in Tijuana are more likely to occur on sandy soils on steep terrain during storm events equal or greater than the threshold precipitation typically required to produce rainfall-runoff gullies on unpaved roads \(Figure 2\).](#) Such estimates would not likely be applicable outside of the LLCW, but the photogrammetric methods deployed here to monitor sediment generation are easily transferrable to other systems, and data on sediment generation from multiple sites would provide a basis for improved understanding and possibly transferrable models.

#### 4.3 Feedbacks between [urbanization processes](#), erosion and slope instabilities from WRIFs: opportunities for hazard mitigation

Erosion and hazards produced by WRIFs were either exacerbated or triggered by erosion during storm events. The observed landslide was triggered by a storm event, but the event was preceded by the water main leak. The observed mega-gullies formed after local runoff initially undermined water mains, which then broke and discharged water onto the hillside, triggering more severe gully erosion. This suggests that WRIFs, storm events, and slope instabilities are interdependent. Moreover, this opens the possibility of reducing mass movement hazards through improved design, management and oversight of water resources infrastructure. Whereas rapid urbanization is broadly linked to minimal levels of governance and institutional oversight of urban infrastructure, especially in least-developed countries (Borelli et al., 2018), water resources infrastructure benefit from relatively high levels of planning, design, engineering and oversight (Whittington et al., 2009; Cook, 2011). For example, mass movement hazards could be reduced by aligning water mains away from topographic low spots susceptible to gully formation, and away from hillslopes that may be susceptible to creeping displacements that stress pipes and cause leaks. Pipeline specifications could also be changed to promote greater ductility, or resistance to failure, under hillslope displacement (Honegger et al., 2010; Han et al., 2012). In turn, the water resources infrastructure would benefit from fewer leaks and breaks and higher levels of reliability.

465 The decadal development of the urban surface is a critical control on the occurrence of WRIFs. While other studies  
highlighted mega-gullies that develop over years and decades, our mega-gullies developed over single storm events with little  
or no latency between urbanization and formation, and pose significant “abrupt” hazards to the population. The spatial location  
of the WRIFs is governed by the temporal sequence of urbanization and land cover transformation that occurs over decades  
(Biggs et al. 201). In Tijuana, mega-gullies occurred on unpaved roads in relatively recently urbanized areas (< 20 years urban)  
470 in the poor periphery, where the water distribution network was buried ~0.5-1m below the surface and easily undermined by  
rainfall-runoff erosion of the unpaved road. Satellite observations suggest roads remain unpaved for decades following  
urbanization in Tijuana (Biggs et al. 2010), with consequent chronic exposure of the community to WRIFs. Roads are gradually  
paved over several decades, starting with the main transit corridors and followed by smaller roads in residential neighborhoods.  
As the network is paved, the water distribution network is more protected from road destruction during storm events. We thus  
475 anticipate that the occurrence of mega-gullies due to WRIFs will become less common with buildout and road paving but could  
remain a chronic problem in marginalized neighborhoods on the urban periphery, where socioeconomic status is low (Biggs  
et al. 2014). The landslide, by contrast, occurred in an area that had been urbanized for longer (~40 years); this kind of hazard  
could occur in older and wealthier neighborhoods on steep slopes if the water supply network develops leaks (Oliva-González  
et al., 2014). While other factors such as overloading by heavy construction and water towers may contribute to landslides in  
480 some urban contexts, the buildings in our study were single story single family residential units with minimal foundations and  
likely small impact on landslide risk (Demoulin et al. 2021). Rather, overloading by soil moisture from WRIFs was likely the  
trigger of the landslide in Tijuana.

#### 4.4 Implications for hazard mitigation in other urban contexts

485 We provide the first-ever documentation of abrupt mega gully formation by water infrastructure failure in an urban  
environment. Such WRIF mega gullies may be under-reported due to their occurrence in the poor urban periphery, and more  
research is needed to support sustainable, safe, and equitable urban environments for the poor. Landslides and mega-gullies  
like those observed in Tijuana have been reported across cities in middle and low-income countries where unregulated  
settlement occurs on steep hillslopes (e.g. landslides by Anderson et al., 2014), but also in developed countries. For example,  
in the city of San Diego, California (USA), soil erosion caused by a storm on January 5, 2016 undermined a 30-foot section of  
490 sewer causing failure and prompting a spill of more than 6.7 million gallons of untreated sewage that severely eroded the  
riverbank and negatively impacted downstream ecosystems (Garrick, 2020). Nevertheless, what is clear is that even though  
the sample size of events reported in this analysis is small, the severity of the eventshazards involving WRIFs is high. Housing,  
transportation, and utilities that serve hundreds of people living in the watershed are impacted by WRIFs in Tijuana, and such  
conditions are likely to occur throughout the poor urban periphery, contributing to the vulnerability of marginalized  
495 populations to environmental hazards. WRIF-based mass movements also contributed a significant amount of sediment to the  
total watershed load, which negatively impacted habitat and aquatic ecosystems, and further increased downstream  
infrastructure maintenance costs (Brand et al., 2020). Acknowledging the challenges of monitoring, as addressed here, what



becomes clear is a need for more widespread monitoring of landslides and mega-gullies and documentation regarding the role of WRIFs. It is possible that a substantial fraction of the most hazardous mass movement events in cities are linked to WRIFs, and that significant hazard reduction can be realized by addressing WRIFs.

## 5 Conclusions

Urban development in Erosional features within a small (11.6 km<sup>2</sup>) watershed on the urban periphery of Tijuana, Mexico was were monitored for a five-year period to document the occurrence frequency and dimension of mega-gullies and landslides, including sediment volumes. Structure from Motion (SfM) photogrammetric techniques helped to rapidly and safety assess the volume and shape of mega-gullies and landslides. Using imagery collected by either Unmanned Aerial Systems (UASs) or a camera on a hand-held pole, SfM techniques registered Digital Surface Models (DSMs) with errors of ~3 cm horizontal RMSE and ~5 cm vertical RMSE which are in line with the needs for sediment budget applications. The methods presented here has the potential to be applied in other rapidly urbanizing watersheds throughout the world.

Over a five-year period with 14 storm events, two mega-gullies and one landslide were observed—and each occurring during a rainfall event. While the link between rainfall and erosion hazards is well known, monitoring showed observations and interviews with residents indicated that all three events were associated with a Water Resources Infrastructure Failure (WRIF). Mega-gullies occurred after a break in a water supply pipe, which unleashed a highly erosive, high-velocity water jet onto an erodible hillslope, destroying an unpaved road and interrupting water supply for weeks. Moreover, pipe breaks were observed to occur after rainfall and runoff formed a small gully that undermined shallow structural support for the water supply pipe. Hence, mega-gullies formed from the observed WRIF-based mega-gully formation can be characterized by the following a two-step process: (1) a

(1) A water supply pipe breaks after the formation of a rainfall-generated gully, and (2) a network.

(2) A mega-gully is formed from the high velocity jet out of the broken water supply pipe. The line.

and the observed WRIF-based landslide was also linked to a formation can be characterized by the following two-step process:

(1) a

(1) A water main leak saturated the hillslope creating the preconditions for a landslide, and (2) heavy.

(2) Heavy rainfall triggered the landslide.

Erosional features caused by WRIFs were larger than features generated by local rainfall and runoff, produced a significant amount of sediment on an event basis, and presented major safety hazards to downstream communities and ecosystems at the neighborhood and watershed scale. The limited data suggest that WRIF-based erosion events occur with an annual frequency of 40-60%, which is far higher than typical design standards for stormwater infrastructure (5-10% annual exceedance probability). Modeling shows that WRIFs contribute, on average, 5% of the total annual sediment generation at the watershed scale, and up to 58% on a storm-event basis. Additional research is needed to improve estimates of the spatial and temporal frequency of erosional features caused by WRIFs, and to understand the significance of WRIF hazards at other spatial and

530 temporal scales and in other geographic contexts. Furthermore, the hazards posed by WRIFs within development on steep terrain calls for greater attention to infrastructure design and maintenance. [While the sample size of this study is small, the results suggest that poorly maintained water distribution networks on the marginalized urban periphery can be the single most important process generating earth surface hazards, and this finding calls for further investigation into the prevalence of these mechanisms elsewhere. These results also point to opportunities for hazard reduction within urban peripheries through improved planning, design and maintenance of water distribution infrastructure.](#)

~~Structure from Motion (SfM) photogrammetric techniques helped to rapidly and safely assess the volume and shape of mega-gullies and landslides. Using imagery collected by either Unmanned Aerial Systems (UASs) or a camera on a hand-held pole, SfM techniques registered Digital Elevation Models (DEMs) with errors of ~3 cm horizontal RMSE and ~5 cm vertical RMSE which are in line with the needs for sediment budget applications.~~

#### **Authors contribution**

NG undertook data acquisition, processing and interpretation of the data, and prepared the manuscript with contributions from all co-authors. BS, TB and AG designed the research, and RB provided valuable guidance on the soil erosion modelling.

#### **Competing interest**

545 The authors declare that they have no conflicts of interest.

#### **Acknowledgements**

This study was funded by National Oceanic and Atmospheric Administration Ecological Effects of Sea Level Rise Program (award NA16NOS4780206), and the US Environmental Protection Agency (EPA) (Interagency Agreement ID # DW-12-92390601-0). The statements, findings, conclusions, and recommendations are those of the author(s) and do not necessarily reflect the views of NOAA or USEPA. We thank Kristine Taniguchi-Quan, Alejandro Hinojosa, Sergio Arregui, and Belinda Sandoval whose support on field collection and data analysis is gratefully acknowledged. We also thank Tijuana Metropolitan Planning Institute (IMPLAN) for data sharing. Special thanks to residents of Los Laureles Canyon, who provided valuable help for data collection.

#### **References**

555 [Adediji, A., Jeje, L. K., and Ibitoye, M. O.: Urban development and informal drainage patterns: Gully dynamics in Southwestern Nigeria, Applied Geography, 40, 90–102. <https://doi.org/10.1016/j.apgeog.2013.01.012>, 2013.](#)

- Alfonso-Torreño, A., Gómez-Gutiérrez, A., Schnabel, S., Lavado-Contador, J. F., de San Jose-Blasco, J. J., and Sánchez-Fernandez, M.: sUAS, SfM-MVS photogrammetry and a topographic algorithm method to quantify the volume of sediments retained in check-dams, *Sci. Total Environ.*, 678, 369-382, <https://doi.org/10.1016/j.scitotenv.2019.04.332>, 2019.
- 560 Anderson, M. G., Holcombe, E., Holm-Nielsen, N., and Della Monica, R.: What Are the Emerging Challenges for Community-Based Landslide Risk Reduction in Developing Countries?, *Nat. Hazards Rev.*, 15(2), 128–139, [https://doi.org/10.1061/\(ASCE\)NH.1527-6996.0000125](https://doi.org/10.1061/(ASCE)NH.1527-6996.0000125), 2014.
- [Archibold, O. W., Levesque, L. M. J., de Boer, D. H., Ashmore, P.: Towards a sociogeomorphology of rivers, \*Geomorphology\*, 251, 149–156, <https://doi.org/10.1016/j.geomorph.2015.02.020>, 2015.](https://doi.org/10.1016/j.geomorph.2015.02.020)
- 565 [Aitken, A. E., and Delanoy, L.: Gully retreat in a semi-urban catchment in Saskatoon, Saskatchewan, \*Applied Geography\*, 23, 261–279. <https://doi.org/10.1016/j.apgeog.2003.08.005>, 2003.](https://doi.org/10.1016/j.apgeog.2003.08.005)
- [Bianchini, S., Raspini, F., Ciampalini, A., Lagomarsino, D., Bianchi, M., Bellotti, F., and Casagli, N.: Mapping landslide phenomena in landlocked developing countries by means of satellite remote sensing data: the case of Dilijan \(Armenia\) area, \*Geomatics, Natural Hazards and Risk\*, 8:2, 225-241, DOI: 10.1080/19475705.2016.1189459, 2017.](https://doi.org/10.1080/19475705.2016.1189459)
- 570 Biggs, T. W., Atkinson, E., Powell, R., and Ojeda-Revah, L.: Land cover following rapid urbanization on the US–Mexico border: Implications for conceptual models of urban watershed processes, *Landscape Urban Plan.*, 96(2), 78–87, <https://doi.org/10.1016/j.landurbplan.2010.02.005>, 2010.
- Biggs, T. W., Anderson, W. G., and Pombo, O. A.: Concrete and Poverty, Vegetation and Wealth? A Counterexample from Remote Sensing of Socioeconomic Indicators on the U.S.–Mexico Border, *The Professional Geographer*, 1–14, <https://doi.org/10.1080/00330124.2014.905161>, 2014.
- 575 Biggs, T. W., Taniguchi, K. T., Gudino-Elizondo, N., Langendoen, E. J., Yuan, Y., Bingner, R. L., and Liden, D.: Runoff and Sediment Yield on the US-Mexico Border, Los Laureles Canyon, US Environmental Protection Agency, Report: EPA/600/R-18/365, Washington, DC, USA, 2018. Available online: [https://cfpub.epa.gov/si/si\\_public\\_record\\_report.cfm?dirEntryId=343214&Lab=NERL](https://cfpub.epa.gov/si/si_public_record_report.cfm?dirEntryId=343214&Lab=NERL), last access: October 3, 2020, 2017.
- 580 Bingner, R. L., Theurer, F. D., Yuan, Y., and Taguas, E.: AnnAGNPS Technical Processes, Washington, D.C. US Department of Agriculture (USDA)—Agricultural Research Service (ARS), Available online: [https://www.wcc.nrcs.usda.gov/ftpref/wntsc/H&H/AGNPS/downloads/AnnAGNPS\\_Technical\\_Documentation.pdf](https://www.wcc.nrcs.usda.gov/ftpref/wntsc/H&H/AGNPS/downloads/AnnAGNPS_Technical_Documentation.pdf), last access: 5 July 2020, 2015.
- Borelli, S., Conigliaro, M., Quaglia, S., and Salbitano, F.: Urban and Peri-urban agroforestry as multifunctional land use.
- 585 Agroforestry: Anecdotal to Modern Science, *Springer Nature*, Singapore, 705-725, [https://doi.org/10.1007/978-981-10-7650-3\\_28](https://doi.org/10.1007/978-981-10-7650-3_28), 2018.
- Brand, M. W., Gudiño-Elizondo, N., Allaire, M., Wright, S., Matson, W., Saksa, P., and Sanders, B. F.: Stochastic Hydro-Financial Watershed Modeling for Environmental Impact Bonds, *Water Resour. Res.*, 56, <https://doi.org/10.1029/2020WR027328>, 2020.

- 590 Calvello, M., Papa, M. N., and Pratschke, J.: Landslide risk perception: a case study in Southern Italy, *Landslides*, 13(2), 349–360, DOI 10.1007/s10346-015-0572-7, 2016.
- Carrera-Hernández, J. J., Levresse, G., and Lacan, P.: Is UAV-SfM Surveying Ready to Replace Traditional Surveying Techniques?, *Int. J. Remote Sens.*, 41 (12), 4818–4835, DOI:10.1080/01431161.2020.1727049, 2020.
- Castillo, C., James, M. R., Redel-Macías, M. D., Pérez, R., and Gómez, J. A.: SF3M software: 3-D photo-reconstruction for non-expert users and its application to a gully network, *The Soil*, 1, 583–594, <https://doi.org/10.5194/soil-1-583-2015>, 2015.
- 595 Castillo, C., and Gómez, A.: A century of gully erosion research: Urgency, complexity and study approaches, *Earth-Science Reviews*, 160, 300–319, <https://doi.org/10.1016/j.earscirev.2016.07.009>, 2016.
- Cook, P.: Infrastructure, rural electrification and development. *Energy Sustain. Dev.*, 15, 304–313. <http://dx.doi.org/10.1016/j.esd.2011.07.008>, 2011.
- 600 Davis, M. L. (Eds): Planet of Slums, Verso, New York, USA, 2006.
- Costa, C. W., Lorandi, R., de Lollo, J. A., Imani, M., and Dupas, F. A.: Surface runoff and accelerated erosion in a peri-urban wellhead area in southeastern Brazil. *Environ Earth Sci*, 77, 160. <https://doi.org/10.1007/s12665-018-7366-x>, 2018.
- Criqui, L.: Infrastructure Urbanism: Roadmaps for Servicing Unplanned Urbanisation in Emerging Cities. *Habitat International* 47: 93–102. <http://dx.doi.org/10.1016/j.habitatint.2015.01.015>, 2015.
- 605 de Albuquerque, A. O., de Carvalho Júnior, O. A., Guimaraes, R. F., Gomes, R. A. T., Hermuche, P. M.: Assessment of gully development using geomorphic change detection between pre- and post-urbanization scenarios. *Environ. Earth Sci*. 79, 232. <https://doi.org/10.1007/s12665-020-08958-9>, 2020.
- Demoulin, A., and Hans-Balder, H.: Causes and Triggers of Mass-Movements: Overloading. *Treatise on Geomorphology (2021): in-press*.
- 610 Dietrich, J. T.: Riverscape mapping with helicopter-based Structure from-Motion photogrammetry, *Geomorphology*, 252, 144–157, <https://doi.org/10.1016/j.geomorph.2015.05.008>, 2016.
- Eltner, A., Kaiser, A., Castillo, C., Rock, G., Neugirg, F., and Abellán, A.: Image-based surface reconstruction in geomorphometry – merits, limits and developments. *Earth Surf. Dynam.*, 4: 359–389. <https://doi.org/10.5194/esurf-4-359-2016>, 2016.
- 615 Ercoli, R. F., Matias, V. R. S., Zago, V. C. P.: Urban Expansion and Erosion Processes in an Area of Environmental Protection in Nova Lima, Minas Gerais State, Brazil. *Front. Environ. Sci.*, 8, 52. <https://doi.org/10.3389/fenvs.2020.00052>, 2020.
- Fu, S., Chen, L., Woldai, T., Yin, K., Gui, L., Li, D., Du, J., Zhou, C., Xu, Y., and Lian, Z.: Landslide hazard probability and risk assessment at the community level: A case of western Hubei, China, *Nat. Hazards Earth Syst. Sci.*, 20, 581–601, <https://doi.org/10.5194/nhess-20-581-2020>, 2020.
- 620 Fugazza, D., Scaioni, M., Corti, M., D’Agata, C., Azzoni, R. S., Cernuschi, M., Smiraglia, C., and Diolaiuti, G.: A Combination of UAV and terrestrial photogrammetry to assess rapid glacier evolution and map glacier hazards, *Nat. Hazards Earth Syst. Sci.*, 18, 1055–1071, <https://doi.org/10.5194/nhess-18-1055-2018>, 2018.

- Garrick, D. (2020). San Diego paying \$2.5M fine for 2016 sewage spill in Tecolote Canyon, Mission Bay. The San Diego Union-Tribune, <https://www.sandiegouniontribune.com/>, last access 16 October 2020.
- 625 Gastil, R. G., Phillips, R. Allison, E.: Reconnaissance geology of the State of Baja California, Geological Society of America Memoir 140, 170, <https://doi.org/10.1130/MEM140-p1>, 1975.
- [Gilbert, G. K., Hydraulic-mining debris in the Sierra Nevada, U.S. Geol. Surv. Prof Pap., 105, 154 pp., 1917.](#)
- Goodrich, K. A., Basolo, V., Feldman, D. L., Matthew, R. A., Schubert, J. E., Luke, A., Eguiarte, A., Boudreau, D., Serrano, K., Reyes, A. S. Contreras, S., Houston, D., Cheung, W., AghaKouchak A., and Sanders, B. F.: Addressing Pluvial Flash  
630 Flooding through Community-Based Collaborative Research in Tijuana, Mexico, *Water*, 12(5), 1257, <https://doi.org/10.3390/w12051257>, 2020.
- Griffin, E., and Ford, L.: A model of Latin American city structure, *Geogr. Rev.*, 70(4), 397–422, 1980.
- Gudino-Elizondo, N., Biggs, T. W., Castillo, C., Bingner, R., Langendoen, E., Taniguchi, K., Kretzschmar, T., Yuan, Y., and Liden, D.: Measuring ephemeral gully erosion rates and topographical thresholds in an urban watershed using Unmanned  
635 Aerial Systems and structure from motion photogrammetric techniques, *Land Degrad. Dev.*, 29, 1896 –1905, <https://doi.org/10.1002/ldr.2976>, 2018a.
- Gudino-Elizondo, N., Biggs, T. W., Bingner, R. L., Yuan, Y., Langendoen, E. J., Taniguchi, K. T., Kretzschmar, T., Taguas, E. V., and Liden, D.: Modelling Ephemeral Gully Erosion from Unpaved Urban Roads: Equifinality and Implications for Scenario Analysis, *Geosciences*, 8, 137, <https://doi.org/10.3390/geosciences8040137>, 2018b.
- 640 Gudino-Elizondo, N., Kretzschmar, T., and Gray, S. C.: Stream flow composition and sediment yield comparison between partially urbanized and undisturbed coastal watersheds; case study: St. John, US Virgin Islands, *Environ. Monit. Assess.*, 191:676, <https://doi.org/10.1007/s10661-019-7778-4>, 2019a.
- Gudino-Elizondo, N., Biggs, T. W., Bingner, R. L., Yuan, Y., Langendoen, E. J., Kretzschmar, T., Taguas, E. V., Taniguchi, K. T., and Liden, D.: Modelling Runoff and Sediment Loads in a Developing Coastal Watershed of the US-Mexico Border,  
645 *Water*, 11, 1024, <https://doi.org/10.3390/w11051024>, 2019b.
- Guo, S., Shao, Y., Zhang, T. Q., Zhu, D. Z., and Zhang, Y. P.: Physical modeling on sand erosion around defective sewer pipes under the influence of groundwater, *J. Hydraul. Eng.*, 139(12), 1247–57, [https://doi.org/10.1061/\(ASCE\)Hy.1943-7900.0000785](https://doi.org/10.1061/(ASCE)Hy.1943-7900.0000785), 2013.
- Han, B., Wang, Z., Zhao, H., Jing, H., and Wu, Z.: Strain-Based Design for Buried Pipelines Subjected to Landslides, *Pet. Sci.*, 9 (2), 236–241, DOI:10.1007/s12182-012-0204-y, 2012
- 650 Hardoy, J. E., Mitlin, D., Satterwaite, D. (2nd Edition): *Environmental Problems in an Urbanizing World*, Routledge, London, UK, <https://doi.org/10.4324/9781315071732>, 2013.
- Honegger, D. G., Hart, J. D., Phillips, R., Popelar, C., and Gailing, R. W.: Recent PRCI Guidelines for Pipelines Exposed to Landslide and Ground Subsidence Hazards: Proceedings of the 8th International Pipeline Conference, Calgary, AB, IPC2010-31311, 1-10, 2010.

[Imwangana, F. M., Highland L., and Bobrowsky P. T.: The landslide handbook: a guide to understanding landslides. Reston: US Geological Survey; 2008.](#)

~~[Dewitte, O., Ntombi, M., and Moeyersons, J.: Topographic and road control of mega-gullies in Kinshasa \(DR Congo\). Geomorphology, 217, 131–139. <https://doi.org/10.1016/j.geomorph.2014.04.021>, 2014.](#)~~

660 [Ionita, I., Fullen, M. A., Zglobicki, W., and Poesen, J.: Gully erosion as a natural and human induced hazard, Nat. Hazards 79, DOI: 10.1007/s11069-015-1935-z, 2015.](#)

[Izumida, A., Uchiyama, S., and Sugai, T.: Application of UAV-SfM photogrammetry and aerial lidar to a disastrous flood: repeated topographic measurement of a newly formed crevasse splay of the Kinu River, central Japan, Nat. Hazards Earth Syst. Sci., 17, 1505–1519, <https://doi.org/10.5194/nhess-17-1505-2017>, 2017.](#)

665 [James, L. A., Hodgson, M. E., Ghoshal, S. and Latiolais, M. M.: Geomorphic change detection using historic maps and DEM differencing: the temporal dimension of geospatial analysis. Geomorphology, 137\(1\): 181–198, DOI: 10.1016/j.geomorph.2010.10.039, 2012.](#)

[James, M. R., and Robson, S.: Straightforward reconstruction of 3D surfaces and topography with a camera: Accuracy and geosciences applications, J. Geophys. Res., 117, 1–17, <https://doi.org/10.1029/2011JF002289>, 2012.](#)

670 [James, M. R., and Robson, S.: Mitigating systematic error in topographic models derived from UAV and ground-based image networks, Earth Surf. Process. Landf., 39, 1413–1420, <https://doi.org/10.1002/esp.3609>, 2014.](#)

[James, M. R., Robson, S., d'Oleire-Oltmanns, S., and Niethammer, U.: Optimising UAV topographic surveys processed with structure-from-motion: Ground control quality, quantity and bundle adjustment, Geomorphology, 280, 51–66, <https://doi.org/10.1016/j.geomorph.2016.11.021>, 2017.](#)

675 [James, M. R., Chandler, J. H., Eltner, A., Fraser, C., Miller, P. E., Mills, J. P., Noble, T., Robson, S., and Lane, S. N.: Guidelines on the use of structure-from-motion photogrammetry in geomorphic research, Earth Surf. Process. Landf., 44 \(10\), 2081–2084, <https://doi.org/10.1002/esp.4637>, 2019.](#)

[Kaiser, A., Erhardt, A., Eltner, A.: Addressing uncertainties in interpreting soil surface changes by multitemporal high-resolution topography data across scales. Land Degrad. Dev., 29 \(8\), 2264–2277, <https://doi.org/10.1002/ldr.2967>, 2018.](#)

680 [Kim, K., Kim, J., Kwak, T. Y., and Chung, C. K.: Logistic regression model for sinkhole susceptibility due to damaged sewer pipes, Nat. Hazards, 93: 765–785, <https://doi.org/10.1007/s11069-018-3323-y>, 2018.](#)

[Kjekstad, O., and Highland, L.: Economic and social impacts of landslides. In: Zhou L, Ooi BC, Meng X \(eds\) Landslides—disaster risk reduction. Springer, Berlin, Heidelberg, pp 573–587, 2009.](#)

685 [Kuo, H. L., Lin, G. W., Chen, C. W., Saito, H., Lin, C. W., Chen, H., and Chao, W. A.: Evaluating critical rainfall conditions for large-scale landslides by detecting event times from seismic records, Nat. Hazards Earth Syst. Sci., 18, 2877–2891, <https://doi.org/10.5194/nhess-18-2877-2018>, 2018.](#)

[Lacroix, P., Dehecq, A., and Taibe, E.: Irrigation-triggered landslides in a Peruvian desert caused by modern intensive farming. Nature Geoscience 13, 56–60. DOI:10.1038/s41561-019-0500-x, 2020.](#)

Luke, A., Sanders, B. F., Goodrich, K. A., Feldman, D. L., Boudreau, D., Eguiarte, A., Serrano, K., Reyes, A., Schubert, J. E.,  
690 AghaKouchak, A., Basolo, V., and Matthew, R. A.: Going beyond the flood insurance rate map: insights from flood hazard  
map co-production, *Nat. Hazards Earth Syst. Sci.*, 18(4), 1097-1120, <https://doi.org/10.5194/nhess-18-1097-2018>, 2018.

Ma, S., Wei, J., Xu, C., Shao, X., Xu, S., Chai, S., and Cui, Y.: UAV survey and numerical modeling of loess landslides: an  
example from Zaoling, southern Shanxi Province, China, *Nat. Hazards*, <https://doi.org/10.1007/s11069-020-04207-1>, 2020.

Makanzu Imwangana, F., Dewitte, O., Ntombi, M., and Moeyersons, J.: Topographic and road control of mega-gullies in  
695 Kinshasa (DR Congo). *Geomorphology*, 217, 131–139, <https://doi.org/10.1016/j.geomorph.2014.04.021>, 2014.

Makanzu Imwangana, F., Vandecasteele, I., Trefois, P., Ozer, P., and Moeyersons, J.: The origin and control of mega-gullies  
in Kinshasa (D.R. Congo). *Catena* 125, 38–49. doi:10.1016/j.catena.2014.09.019, 2015.

Marino, P., Peres, D. J., Cancelliere, A., Greco, R., and Bogaard, T. A.: Soil moisture information can improve shallow  
landslide forecasting using the hydrometeorological threshold approach, *Landslides*, DOI: 10.1007/s10346-020-01420-8,  
700 2020.

Mazzoleni, M., Paron, P., Reali, A., Juizo, D., Manane, J., and Brandimarte, L.: Testing UAV-derived topography for hydraulic  
modelling in a tropical environment, *Nat. Hazards*, 103, 139–163, <https://doi.org/10.1007/s11069-020-03963-4>, 2020.

~~Miller, J. R., Ferri, K., Grow, D., and Villarreal, L.: Hydrologic, geomorphic, and stratigraphic controls on suspended sediment  
transport dynamics, Big Harris Creek restoration site, North Carolina, USA, *Anthropocene*, 25,  
705 <https://doi.org/10.1016/j.ancene.2018.12.002>, 2019.~~

McAdoo, B. G., Quak, M., Gnyawali, K. R., Adhikari, B. R., Devkota, S., Rajbhandari, P. L., and Sudmeier-Rieux, K.: Roads  
and landslides in Nepal: how development affects environmental risk, *Nat. Hazards Earth Syst. Sci.*, 18, 3203–3210,  
<https://doi.org/10.5194/nhess-18-3203-2018>, 2018.

~~Miller, J. R., Ferri, K., Grow, D., and Villarreal, L.: Hydrologic, geomorphic, and stratigraphic controls on suspended sediment  
710 transport dynamics, Big Harris Creek restoration site, North Carolina, USA, *Anthropocene*, 25,  
<https://doi.org/10.1016/j.ancene.2018.12.002>, 2019.~~

Minch, A. J., Ashby, J., Deméré, T., and Kuper, T.: Correlation and depositional environments of the Middle Miocene Rosarito  
Beach Formation of northwestern Baja California, Mexico, In: J.A. Minch and J.R. Ashby, Editors, *Miocene and Cretaceous  
depositional environments, northwestern Baja California, Mexico: Pacific Section, American Association of Petroleum  
715 Geologists*, 54, 33-46, 1984.

Moeyersons, J., Makanzu Imwangana, F., and Dewitte, O.: Site- and rainfall-specific runoff coefficients and mega-gully  
development in Kinshasa (DR Congo). *Natural Hazards*, 79(1), 203–233. <https://doi.org/10.1007/s11069-015-1870-z>, 2015.

Nadal-Romero, E., Revuelto, J., Errea, P., and López-Moreno, J. I.: The application of terrestrial laser scanner and SfM  
photogrammetry in measuring erosion and deposition processes in two opposite slopes in a humid badlands area (central  
720 Spanish Pyrenees), *The Soil*, 1, 561–573, <https://doi.org/10.5194/soil-1-561-2015>, 2015.

Monsieurs, E., Dewitte, O., Demoulin, A.: A susceptibility-based rainfall threshold approach for landslide occurrence. *Nat.  
Hazards Earth Syst. Sci.*, 19, 775–789, 2019 <https://doi.org/10.5194/nhess-19-775-2019>, 2019.

- Oliva-González, A. O., Jiménez, D. M., Alvarez-García, I. N., Nicieza, C. G., and Álvarez-Vigil, A. E.: Hillside instability in the Tijuana metropolitan area. Analysis of landslide-provoked building collapse, *Eng. Fail. Anal.*, 46, 166–178, <https://doi.org/https://doi.org/10.1016/j.engfailanal.2014.08.004>, 2014.
- 725 Peng, L., Lin, L., Liu, S. Q., and Xu, D.: Interaction between risk perception and sense of place in disaster-prone mountain areas: A case study in China's Three Gorges Reservoir Area, *Nat. Hazards*, 85(2), 777–792, DOI 10.1007/s11069-016-2604-6, 2017.
- Poesen, J.: Soil erosion in the Anthropocene: Research needs, *Earth Surf. Process. Landf.*, 43(1), 64–84, <https://doi.org/10.1002/esp.4250>, 2018.
- 730 Retief, F., Bond, A., Pope, J., Morrison-Saunders, A., and King, N.: Global megatrends and their implications for environmental assessment practice, *Environ. Impact Assess. Rev.*, 61:52–60, <https://doi.org/10.1016/j.eiar.2016.07.002>, 2016.
- Sepúlveda, S. A., and Petley, D. N.: Regional trends and controlling factors of fatal landslides in Latin America and the Caribbean, *Nat. Hazards Earth Syst. Sci.*, 15(8), 1821–1833, <https://doi.org/10.5194/nhess-15-1821-2015>, 2015.
- 735 Sidle R, Furuichi T, and Kono Y.: Unprecedented rates of landslide and surface erosion along a newly constructed road in Yunnan, China. *Nat. Hazards*, 57, 313–326, DOI: 10.1007/s11069-010-9614-6, 2011.
- Taniguchi, K. T., Biggs, T. W., Langendoen, E. J., Castillo, C., Gudino-Elizondo, N., Yuan, Y., and Liden, D.: Stream channel erosion in a rapidly urbanizing region of the US–Mexico border: Documenting the importance of channel hardpoints with Structure from-Motion photogrammetry, *Earth Surf. Process. Landf.*, 43, 1465–1477, <https://doi.org/10.1002/esp.4331>, 2018.
- 740 USDA (2018). Estimating Moist Bulk Density by Texture. [https://www.nrcs.usda.gov/wps/portal/nrcs/detail/soils/survey/office/ssr10/tr/?cid=nrcs144p2\\_074844](https://www.nrcs.usda.gov/wps/portal/nrcs/detail/soils/survey/office/ssr10/tr/?cid=nrcs144p2_074844), last access: 3 September 2019.
- USGS (2021). Landslide Hazard Information. <https://geology.com/usgs/landslides/>, last access: 22 January 2021.
- Valentin, C., Poesen, J., and Li, Y.: Gully erosion: Impacts, factors and control, *Catena* 63, 132–153, <https://doi.org/10.1016/j.catena.2005.06.001>, 2005.
- 745 Valenzuela, P., Domínguez-Cuesta, M. J., García, M. A. M., and Jiménez-Sánchez, M.: Rainfall thresholds for the triggering of landslides considering previous soil moisture conditions (Asturias, NW Spain), *Landslides*, 15 (2), 273–282, DOI 10.1007/s10346-017-0878-8., 2018.
- Van Zyl, J. E., Alsaydalani, M. O., Clayton, C. R., Bird, T., and Dennis, A.: Soil fluidisation outside leaks in water distribution pipes—Preliminary observations, *J. Water Manage.*, 166(10), 546–555, <https://doi.org/10.1680/wama.11.00119>, 2013.
- 750 [Van Den Eeckhaut, M., Poesen, J., Dewitte, O., Demoulin, a., De Bo, H., Vanmaercke-Gottigny, M.C.: Reactivation of old landslides: Lessons learned from a case-study in the Flemish Ardennes \(Belgium\). \*Soil Use and Management\* 23, 200–211. DOI:10.1111/j.1475-2743.2006.00079.x, 2007.](https://doi.org/10.1111/j.1475-2743.2006.00079.x)
- Vigiak, O., Borselli, L., Newham, L. T. H., McInnes, J., and Roberts, A. M.: Comparison of conceptual landscape metrics to define hillslope-scale sediment delivery ratio, *Geomorphology*, 138, 74–88, <https://doi.org/10.1016/j.geomorph.2011.08.026>, 2012.
- 755



[Vanmaercke, M., Panagos, P., Vanwalleghem, T., Hayas, A., Foerster, S., Borrelli, P., Rossi, M., Torri, D., et al.: Measuring, modelling and managing gully erosion at large scales: a state of the art Earth Sci. Rev., 218, DOI: \[10.1016/j.earscirev.2021.103637\]\(#\), 2021.](#)

760 [Vanmaercke, M., Poesen, J., Van Mele, B., Demuzere, M., Bruynseels, A., Golosov, V., Rodrigues Bezerra, J., Bolysov, S., Dvinskih, A., Frankl, A., Fuseina, Y., Guerra, A., Haregeweyn, N., Ionita, I., Makanzu Imwangana, F., Moeversons, J., Moshe, I., Nazari Samani, A., Niacsui, L., Nyssen, J., Otsuki, Y., Radoane, M., Rysin, I., Ryzhov, Y., Yermolaev, O.: How fast do gully headcuts retreat? Earth-Science Reviews 154, 336–355. \[http://dx.doi.org/10.1016/j.earscirev.2016.01.009\]\(#\), 2016](#)

Weis, D. A., Callaway, J. C., and Gersberg, R. M.: Vertical accretion rates and heavy metal chronologies in wetland sediments of the Tijuana Estuary, Estuaries, 24, 840–850, [https://doi.org/10.2307/1353175](#), 2001.

765 Wheaton, J. M., Brasington, J., Darby, S. E., and Sear, D. A.: Accounting for uncertainty in DEMs from repeat topographic surveys: improved sediment budgets, Earth Surf. Process. Landf., 35, 136–156, [https://doi.org/10.1002/esp.1886](#), 2010.

Whittington, D., Davis, J., Prokopy, L., Komives, K., Thorsten, R., Lukacs, H., Bakalian, A., and Wakeman, W.: How well is the demand-driven, community management model for rural water supply systems doing? Evidence from Bolivia, Peru and 770 Ghana, Water Policy, 11(6): 696-718. DOI: 10.2166/wp.2009.310, 2009.

[Xu, X., Zhang, H., Aldana-Jague, E., Clapuyt, F., Wilken, F., Vanacker, V., and Van Oost, K.: Evaluating the potential of post-processing kinematic \(PPK\) georeferencing for UAV-based structure-from-motion \(SfM\) photogrammetry and surface change detection, Earth Surf. Dynam., 7, 807–827, \[https://doi.org/10.5194/esurf-7-807-2019\]\(#\), 2019.](#)

775 ~~[H., Wang, W., Zhao, C., and Yan, Q.: Quantitative monitoring of gravity erosion using a novel 3D surface measuring technique: validation and case study, Nat. Hazards, 75\(2\), 1927–1939, DOI: 10.1007/s11069-014-1405-z, 2015.](#)~~

Zhuo, L., Dai, Q., Han, D., Chen, N., Zhao, B., and Berti, M.: Evaluation of remotely sensed soil moisture for landslide hazard assessment. IEEE J. Sel. Top. Appl. Earth Obs. Remote Sens., [https://doi.org/10.1109/JSTARS.2018.2883361](#), 2019.

[Zolezzi, G., Bezzi, M., Spada, D., Bozzarelli, E.: Urban gully erosion in sub-Saharan Africa: a case study from Uganda. Land Degrad Dev 29\(3\):849–859. \[https://doi.org/10.1002/ldr.2865\]\(#\), 2018.](#)